Nanometer-Sized Molybdenum–Iron Oxide Capsule-Surface Modifications: External and Internal

Achim Müller, Hartmut Bögge, Filipa L. Sousa, Marc Schmidtmann, Dirk G. Kurth, Dirk Volkmer, Joris van Slageren, Martin Dressel, Melissa L. Kistler, and Tianbo Liu**

The cluster *$\{(Mo)Mo_5\}_{12}Fe^{III}_{30}$* ***1a*** *present in compound* ***1*** *(cluster diameter ≈2.3 nm), which belongs to the family of nanoscale spherical porous $\{(Mo)Mo_5\}_{12}\{Linker\}_{30}$ capsules that allow a new type of nanochemistry inside their cavities as well as unprecedented aggregation processes under gaseous, solution, and solid-state conditions, is the starting material for the present investigation. In solution it reacts with $LnCl_3{\cdot}nH_2O$ (Ln = Ce, Pr) thereby replacing six Fe^{III} ions with Ln^{III} ions to form compounds* ***2*** *(Ce) and* ***3*** *(Pr). During metal-cation exchange, some of the pentagonal $\{(Mo)Mo_5O_{21}(H_2O)_6\}^{6-}$ units, which are connected to the Fe^{III} centers in* ***1a****, decompose, thus leading to a temporary capsule opening and uptake of the formed smaller molybdate units into the capsule cavities. In* ***2*** *and* ***3****, the pentagonal units are connected via 24 Fe^{III} and six Ln^{III}-type linkers/spacers representing together the capsule skeletons, which are structurally well-defined in contrast to the capsule contents. The new capsules self-associate into single-layer blackberry-type structures, thus extending the variety of these types of assemblies; the assembly process, that is, the size of the final species, can be controlled by the pH, which allows the generation of differently sized nanoparticles. Magnetic properties of the two new nanomaterials* ***2*** *and* ***3*** *are also determined.*

Keywords:
- magnetic properties
- metal oxides
- molybdenum
- nanomanipulation
- self-assembly

[*] Prof. A. Müller, Dr. H. Bögge, F. L. Sousa, M. Schmidtmann
Fakultät für Chemie der Universität
Postfach 100131
33501 Bielefeld (Germany)
Fax: (+49) 521-106-6003
E-mail: a.mueller@uni-bielefeld.de
Dr. D. G. Kurth
Max Planck-Institute of Colloids and Interfaces
14424 Potsdam (Germany)
Prof. D. Volkmer
Anorganische Chemie II, Universität Ulm
Albert-Einstein-Allee 11
89081 Ulm (Germany)
Dr. J. vanSlageren, Prof. M. Dressel
1. Physikalisches Institut, Universität Stuttgart
Pfaffenwaldring 57
70550 Stuttgart (Germany)
M. L. Kistler, Prof. T. Liu
Department of Chemistry, Lehigh University
Bethlehem, PA 18015 (USA)
Fax: (+1) 610-758-6536
E-mail: til204@lehigh.edu

1. Introduction

The intentional synthesis of nanoscopic multifunctional materials that combine porosity with other desired properties reveals a challenge of contemporary chemistry and nanoscience.[1] Though in numerous studies porous three-dimensional inorganic networks have been successfully investigated,[1d] the related research on discrete porous nanomaterials, especially those with structurally well-defined external and internal surfaces, is very limited. An exception to this are the nanosized spherical capsules with pentagonal molybdenum-oxide-based units, that is, of the type $\{Pentagon\}_{12}\{Linker\}_{30}$, which show the construction principles of a football; the linkers can be either mononuclear $\{M\}$[2] or dinuclear metal-cation-type units $\{M_2\}$.[3] In the case of $M = Fe^{III}$ (the starting material for the present reactions)[2] – exhibiting a nanosized cavity and a hydrophilic surface with a variety of structural features – the surface functionalities can be varied in a well-defined way. The cor-

responding clusters behave as weak nanoacids due to the presence of H_2O ligands coordinated to Fe^{III} ions. While they exist in the form of discrete, neutral molecules in aqueous solution at lower pH values, they become deprotonated at higher pH values, which leads to a new type of assembly process. Remarkably, the process can be controlled simply by varying the pH values, which allows the deliberate generation of differently sized nanoparticles, a long-term goal in nanoscience;[4] see also Ref. [5], which refers to unusual magnetic properties.

Herein we report on the partial substitution of some of the Fe^{III} linkers by Ln^{III} (=Ce^{III}, Pr^{III}) cations.[6] This approach can be discussed in the sense that 30 exchangeable metal cations {M} are trapped in a spherical matrix built up by 12 pentagonal molybdenum-oxide-based units of the type {(Mo)Mo_5}, while the central (Mo) atoms span an icosahedron and the 30 {M} centers form an icosidodecahedron.[9] Due to the partial metal–metal cation replacements, which can easily be performed and lead in the present case to well-defined spherical skeletons of the type $\{(Mo)Mo_5\}_{12}M_{30}$, a temporary capsule opening occurs. The process allows uptake of quite a number of "molybdate units" and Ln^{III} ions from the capsule exterior into the capsule interior.

2. Results and Discussion

After adding aqueous solutions of $CeCl_3{\cdot}7H_2O$ or $PrCl_3{\cdot}6H_2O$ to an aqueous solution of **1** (containing the cluster **1a**; see formula), compounds **2** and **3** exhibiting the above-mentioned metal-cation replacements precipitate in a crystalline form (see Experimental Section). Both were characterized by analyses (including ESCA and ICP-MS for the metals), thermogravimetry (to determine the actual crystal water content and the thermal stability), spectroscopy (IR, Raman, UV/Vis, and ^{57}Fe Mössbauer) and single-crystal X-ray structure analyses[10] (including bond valence sum (BVS) calculations).

$[Mo_{72}Fe_{30}O_{252}(CH_3COO)_{12}$
$\cdot\{Mo_2O_7(H_2O)\}_2$
$\cdot\{H_2Mo_2O_8(H_2O)\}(H_2O)_{91}] \equiv \mathbf{1a}$;

$\mathbf{1a} \cdot$ ca. $150\,H_2O \equiv \mathbf{1}$[2a,11]

[Capsule content $\subset$ $\{Mo_{72}Fe_{24}Ln_6O_{252}(H_2O)_{105}\}$]·ca. $200\,H_2O \equiv \mathbf{2}$ (Ln=Ce), **3** (Ln=Pr); capsule content: ca. $Mo_{18}O_{66}Ln_2(H_2O)_n$;[11b] see Figure 2, and Experimental Section.

Compounds **2** and **3** crystallize in the space group $R\bar{3}c$ and contain besides crystallized water the discrete spherical clusters **2a** and **3a** (**2** and **3** without crystal water; see Figure 1, top left). These are – as with **1a** (Figure 1, top right) – built up by 12 pentagonal units of the type $\{(Mo)Mo_5O_{21}(H_2O)_6\}^{6-}$ exhibiting a central bipyramidal $\{MoO_7\}$ group linked to five edge-sharing $\{MoO_6\}$ octahedra. Due to the partial metal-linker replacements the pentagonal units in **2a** and **3a** are connected via 24 Fe^{III} and six Ln^{III}-type linkers/spacers. Whereas in compounds **2** and **3** the structure of the skeleton is well defined (Figure 1, top left), this is not the case for the capsule contents (Figure 2). While the Fe^{III} centers in **2a** and **3a** occupy the same type of sites as in **1a** (Figure 1) the six Ln^{III} centers – positioned at 12 sites with an occupancy of 50% – lie slightly above the pore area (Figure 2, bottom) and are coordinated by O atoms in form of a tricapped trigonal prism, which includes five H_2O ligands. Both types of linker ions are also connected to four oxygen atoms of two $\{MoO_6\}$ octahedra belonging

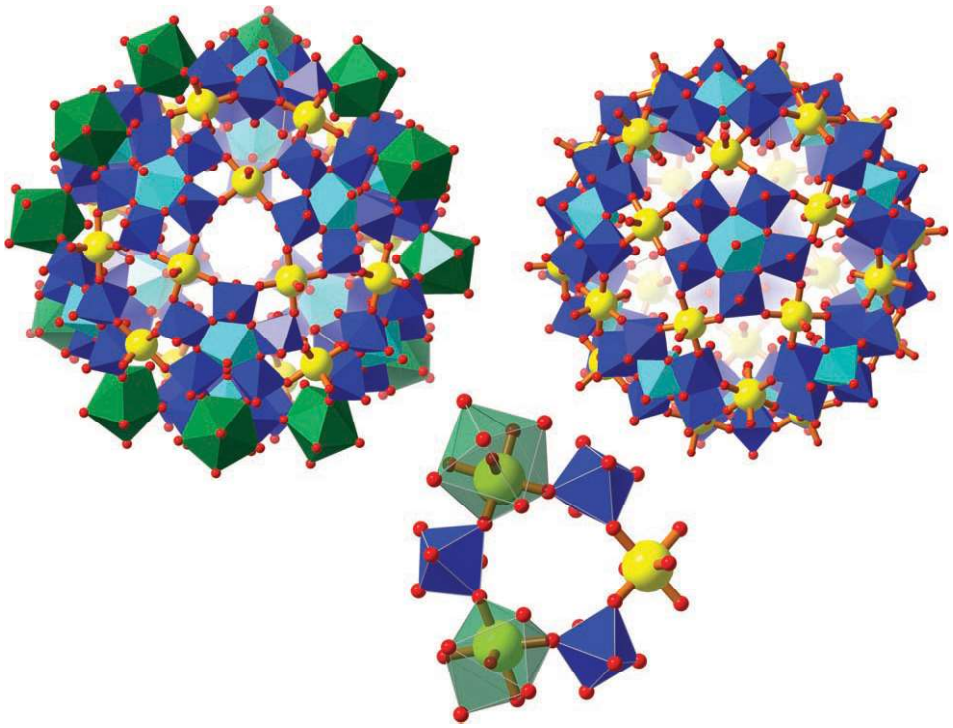

Figure 1. Top left: Combined polyhedral and ball-and-stick representation of the well-defined skeletal surface structures of **2a** and **3a** (viewed in the direction of the C_3 axis) emphasizing besides the basic pentagonal units {(Mo)Mo_5} (in blue, central MoO_7 unit in turquoise) and the $Fe(H_2O)^{3+}$ linkers (Fe: yellow, O: red), the hydrated Ln^{III} (green polyhedra). As the six Ln^{III} are positioned disordered on 12 positions with 50% occupation, all 12 LnO_9 polyhedra are shown. Top right: Structure of (only) the skeleton of the initial spherical capsules **1a** highlighting the basic pentagonal units in a polyhedral representation and the 30 Fe^{III} linker-type centers in octahedral environments with two bonds to water ligands (or to one external H_2O and one to an internal acetate) and four bonds to two different pentagonal units (internal ligands are not shown; color code as above). Bottom: Demonstration of the Fe^{III} substitutions by Ln^{III}; one pore of **2a** or **3a** is shown according to 50% Ln^{III} and 50% Fe^{III} occupancy (color code as above).

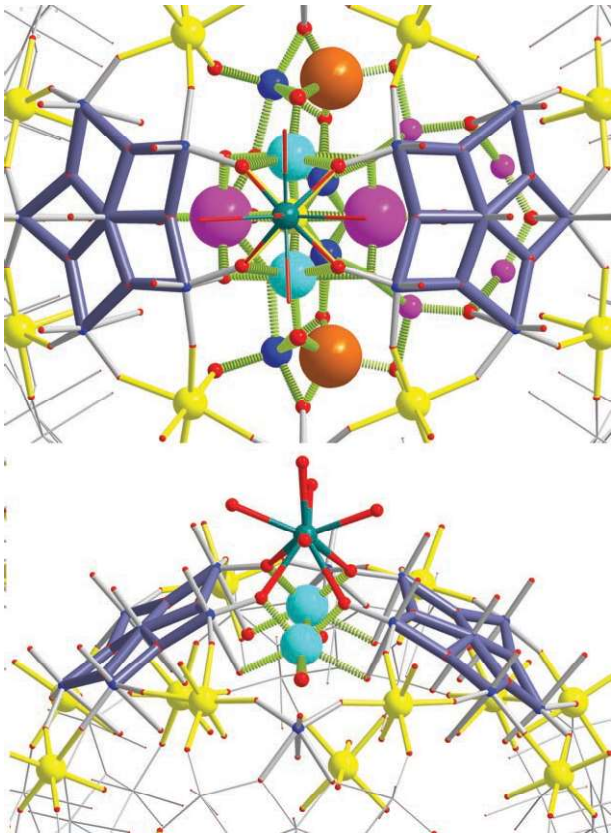

Figure 2. The capsule interior of **2a** and **3a** contains 18 molybdenum–oxide-based units (disordered probably because of the short opening time). Top: Combined ball-and-stick and wireframe representation of a segment highlighting two {(Mo)Mo_5} units (dark grey sticks), the mononuclear MoO_4^{2-} units (Mo: orange), as well as three different additional types of mono/dinuclear molybdenum–oxide units (Mo: pink, turquoise (both with larger spheres according to larger occupancies) and blue) coordinated to certain parts of the inner cavity shell (other color codes as in Figure 1). Bottom: Combined ball-and-stick/wireframe representation of a part of the skeletal structure of **2a** and **3a** emphasizing especially the hydrated Ln^{III} (green) of a pore area where Fe^{III} cannot reside. Additionally shown is one of the above-mentioned "Mo-type units" (turquoise; only positioned there in case of the presence of Ln^{III} and not of Fe^{III}).

to two neighboring pentagonal units (Figure 1, top left and right).

Remarkably, the partial exchange of Fe^{III} by Ln^{III} ions leads to a decomposition of some of the {(Mo)Mo_5O_{21}-$(H_2O)_6$}$^{6-}$ units, which are connected to the Fe^{III} centers and are subsequently replaced. The decomposition occurs because the pentagonal units are – due to their relatively high negative charge – not stable as discrete entities and only if they are embedded in a protecting, that is, charge-reducing environment, as for example in **1a**. All observations infer that a partial opening of the initial cluster capsule **1a** occurs, which leads not only to a practically complete release of acetate ligands but also to the incorporation of several "new molybdate-type" species – formed from the pentagonal units – into the cavity. The reason for the preferred incorporation of these units is that the capsule skeletons of the clusters **1a**, **2a**, **3a**, as well as **4a** (with a discrete encapsulated guest) and **5a**[12] are positively charged: the total skeletal charge of +18 results from that of all the pentagonal units (12×(−6)=−72) and that of the spacers (30×(+3)=+90). The positive charge in **1a** is partially neutralized by the weakly bound acetate ligands, but these ligands are nearly completely released during capsule opening and are therefore absent in **2** and **3**. In the latter two compounds the skeletal charge is compensated essentially by the encapsulated molybdate-type units, which possess negative charges.[11b] The fact that analyses showed (within the error limit) no additional cations in the crystal lattice of **2** and **3** proves the neutrality of the clusters while taking into account the two additional encapsulated Ln^{III} cations (see formula). An interesting variant of clusters **1a**, **2a**, and **3a** exists in case of **4a**, which shows an encapsulated well-defined discrete $\{Mo_6O_{19}\}^{2-}$ cluster, that is, an encapsulated species not interacting with the skeleton, as is the case with **2** and **3**.

$$Na_4[[Mo_6O_{19}]^{2-} \subset \{Mo_{72}Fe_{30}O_{252}(CH_3COO)_{20}(H_2O)_{92}\}] \equiv \mathbf{4};$$

$$\mathbf{4a} \cdot \text{ca. } 120\,H_2O \equiv \mathbf{4}^{[2c]}$$

$$[H_4Mo_{72}Fe_{30}O_{254}(CH_3COO)_{10}\{Mo_2O_7(H_2O)\}$$
$$\cdot\{H_2Mo_2O_8(H_2O)\}_3(H_2O)_{87}] \equiv \mathbf{5a};$$

$$\mathbf{5a} \cdot \text{ca. } 80\,H_2O \equiv \mathbf{5}^{[12]}$$

What does the capsule cavity interior of **2a** and **3a** look like? The following description is simplified because of the complicated disorder of the molybdenum atoms inside the related capsules together with the corresponding low occupancies, a scenario that does not allow a straightforward positioning of the related O atoms by X-ray crystallography. Approximately three Mo atoms in the form of mono/dinuclear oxide units are found below the positions occupied by the linker-type lanthanide cations (due to the disorder and low occupancy it is difficult to distinguish the two different (i.e., mono/dinuclear) types; see Figure 2). Furthermore, six mononuclear {MoO_4^{2-}} units – sharing two oxygen atoms with the metal centers of the hexagonal {$Mo_3LnFe_2O_6$} pores – are present, as well as approximately nine further molybdenum atoms also in form of mono/dinuclear oxide units (see remarks above and Figure 2). Whereas all of the Mo-based units are attached to the inner shell of the positively charged skeletons of **2a** and **3a** this is not the case for the two further disordered Ln^{III} cations found in the more central part of the cavities (see formulas). These cations contain water ligands as well as four bridging oxygen atoms shared with the above-mentioned molybdenum–oxide-type units. The rest of the cavity is filled with disordered H_2O molecules, the exact number of which cannot be determined. The different types of water molecules of **2** and **3** show different "behavior" upon heating, as expected. Whereas the crystallized water is released at around 105 °C (≈17 % weight loss), which does not influence the stability

of capsules **2a** and **3a**, this is, as expected, different for the release of coordinated (constitutional) water molecules appearing in a first step at $\approx 300\,^{\circ}C$ (weight loss $\approx 6\%$; for stabilization options see below).

The solid-state Raman spectra of **2** and **3** show a splitting of the band corresponding to the symmetric breathing vibration of the Mo=O bonds, which is observed at 950 cm^{-1} in **1**. The splitting of this band results from the lower capsule symmetry of **2a** and **3a**. In addition, the ^{57}Fe Mössbauer spectrum of **2** measured at 293 K also shows symmetry lowering, and correspondingly the presence of Fe^{III} centers in two different types of sites ($\delta = 0.37(4)\ mm\,s^{-1}$, $\Delta E_Q = 0.996(11)\ mm\,s^{-1}$ and $\delta = 0.39(2)\ mm\,s^{-1}$, $\Delta E_Q = 0.564(12)\ mm\,s^{-1}$) with a relative contribution of approximately 25% and 75%, respectively. This is explained by considering that the coordination sites/environments of the Fe centers at the linker positions are not equal in **2**, which is the case for **1** ($\delta = 0.52(1)\ mm\,s^{-1}$, $\Delta E_Q = 0.72(1)\ mm\,s^{-1}$ at 4.2 K[2a,13]).

To characterize the magnetic properties of **2** and **3**, the magnetic susceptibility versus temperature as well as the magnetization as a function of field was measured (Figure 3). Rare-earth ions are different from most first-row transition-metal ions in that the orbital angular momentum is not quenched, leading, for example, to g values that are widely different from the free-electron value of $g = 2$. In fact, the f^1 Ce^{III} ion has a $^2F_{5/2}$ ground state with $g = 6/7$, and an expected room-temperature χT value of 0.80 $cm^3\,K\,mol^{-1}$, while the f^2 Pr^{III} ion has a $^3H_4$ ground state with $g = 4/5$ and an expected χT value of 1.60 $cm^3\,K\,mol^{-1}$.[14] Due to the low molar χT values compared to typical values for Fe^{III} ($\chi T = 4.375\ cm^3\,K\,mol^{-1}$), the rare-earth ions are expected to contribute only weakly to the overall magnetic susceptibility of **2** and **3**, as shown in Figure 3 where the susceptibility curves look very similar for both complexes: The room temperature χT values (117.17 and 123.65 $cm^3\,K\,mol^{-1}$, for **2** and **3** respectively) are very close to the values calculated for 24 noninteracting Fe^{III} ions and eight rare-earth ions (111.4 and 117.8 $cm^3\,K\,mol^{-1}$ for **2** and **3**, respectively). With decreasing temperature the χT product drops monotonously indicating antiferromagnetic interactions, as also evidenced by the Weiss temperatures of $\theta = -27$ and $\theta = -24$ K obtained from fitting data at $T > 100$ K for **2** and **3**, respectively. The Weiss temperatures are slightly higher, but very similar to that of the parent compound **1** ($\theta = -22$ K), which shows that the exchange interactions involving the rare-earth ions are not much stronger than the Fe…Fe couplings. The magnetization versus field curves (Figure 3, bottom) show an almost linear increase due to occupation of the spin states with progressively larger spin, again similar to **1**. Interestingly, the numerical derivative of the magnetization curve does not show the characteristic minimum observed in **1** within the accessible field range, indicating that the replacement of Fe^{III} by rare-earth ions has influenced the magnetic properties.

The discrete spherical cluster **1a** of the starting compound **1**, which has been shown to be stable in aqueous solution for months,[4a] possesses 30 $\{Fe(H_2O)\}^{3+}$ units at the external surface, which can undergo deprotonation similar

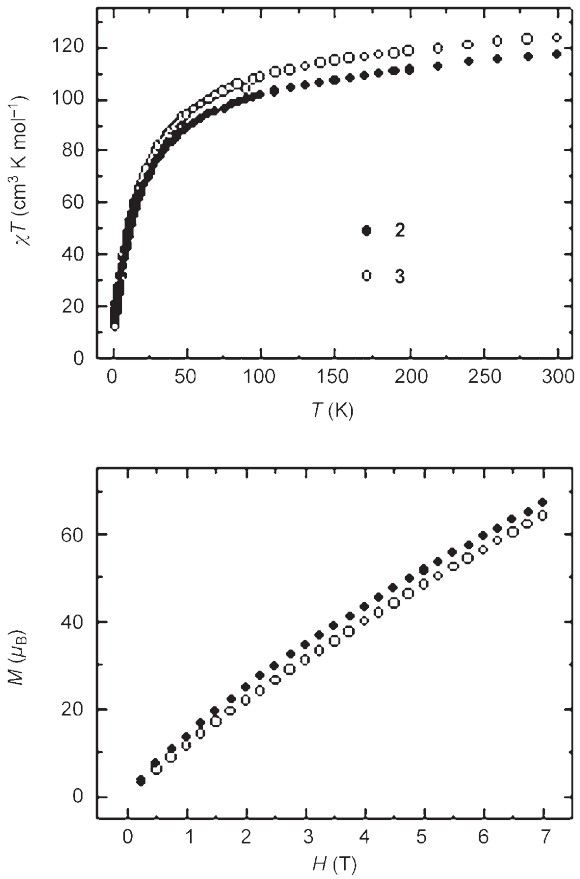

Figure 3. xT as a function of temperature (top) for **2** (●) and **3** (○) and the magnetization as a function of the field (bottom) measured on powder samples.

to the classical complex $[Fe(H_2O)_6]^{3+}$, especially if the pH value is increased. It has been proven that deprotonation is a requirement for the assembly process of the **1a** species into vesicles to take place.[4a] It can now be shown that aqueous solutions of **2** are acidic, due to the deprotonation of the H_2O ligands attached to Fe^{III} centers; for a 0.5 $mg\,mL^{-1}$ solution of **2** the pH is 3.9, that is, an average of 5.3 protons are released from each cluster. But the degree of deprotonation is slightly lower than that of **1a**.[4a] In the light-scattering (DLS) experiment at pH 3.9 (see Experimental Section) it was found that the macroions **2a** self-assemble into spherical, single-layer, vesicle-like "blackberry-type" structures in dilute solution, with an average hydrodynamic radius R_h of around 40 nm (Figure 4), which is slightly larger than those obtained for **1a** under comparable conditions (see, for example, Ref. [4a]). The R_h values measured at different scattering angles show little angular dependence, suggesting that the supramolecular structure must be isotropic, that is, close to spherical. The R_h value of **2a** compared to that of **1a** is reasonable since the size of the present blackberry-type structure is found to be related to the charge of the macroions: larger structures are formed when the macroions carry fewer charges.[4a] As the scanning electron microscopy (SEM) images of the blackberry-type structures formed in aqueous solution of **2a** are very similar

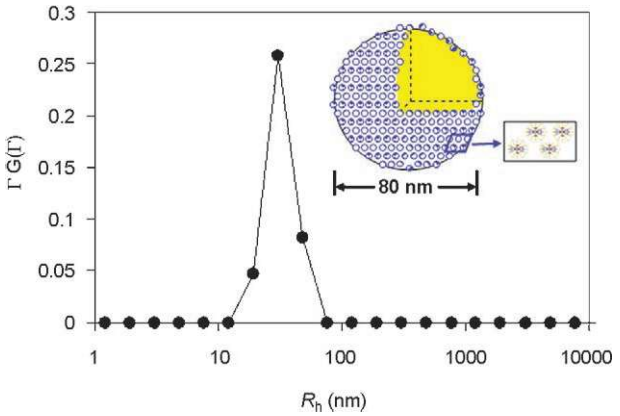

Figure 4. CONTIN analysis of the DLS measurement of a 0.5 mg mL^{-1} solution of **2a**. The measurement was performed at a 90° scattering angle. The inserted cartoon shows the supramolecular structure of the self-assembled macroions **2a**, which is in agreement with the preliminary results and that of **1a**[4] based on sophisticated experiments.

to those of **1a** reported by us recently,[4a] we decided to refer to solvent conditions where **2a** has a lower degree of deprotonation, that is, in 50 vol.% water/acetone, which also allows better images to be taken. As a result, larger blackberry-type structures – as expected – were found, in agreement with DLS measurements (100–500-nm radius, that is, with a broad size distribution). One SEM image of two vesicles is shown (Figure 5) (≈300–350-nm radius). The fact that the new macroions **2a** also self-assemble further infers that the observed unprecedented self-assembly in polar solvents is a universal phenomenon of these types of metal–oxide-based macroions.[4]

3. Conclusions

Aqueous solutions of **1** contain unique monodisperse nanoparticles/capsules with identical mass, shape, size, tunable charges, and well-defined internal/external surface structures. The structure consists of open-shell metal centers that are "trapped" in a spherical matrix built up by 12 pentagonal {(Mo)Mo_5}-type units, which are not stable as discrete entities because of their relatively large negative charge. This has the consequence that decomposition of the pentagonal units attached to the replaced metal centers occurs during the exchange of the Fe^{III} centers with cations such as Ln^{III}, while smaller molybdate units such as $\{MoO_4\}^{2-}$ are formed. The intermediate/temporary opening of the spherical particles leads to, apart from a release of acetate groups, the uptake of the formed "molybdate" units. An interesting aspect is that the extremely complex structure in the capsule cavity of **2** and **3** is the same, which proves the high formation tendency. These results show perspectives for new synthetic routes in the sense that different types of metal cation replacements can be studied, which can lead to different uptake processes in the presence of other negatively charged ions than the molybdates shown in the present case. The corresponding compounds should also show different assembly processes in solution mainly depending on the deprotonations/charges on their external surfaces, which can according to the present result be widely varied. It will be interesting to see how the uptake of species into the interior of POMs will proliferate new concepts in encapsulation chemistry, a major task of our research,[3g,h,7b] and special aspects of catalysis, where molybdenum–oxide systems play a major role,[15a] especially those with pentagonal building blocks referred to here. The present results allow an extension to a variety of other scenarios including those that are of interest for materials science. The uptake of special Ln ions into the M–O framework could lead to interesting fluorescent properties. The well-defined size, the pH- and size-dependent features, and the ability to incorporate the present giant POMs into device architectures,[15b,16] together with their characteristic optical properties makes them potential candidates for various applications including biosensing.[17] There is the option to stabilize these special hollow clusters in silica matrices, even with an option to generate channels to the embedded clusters.[18] In addition, the above-mentioned assembly process of this type of POM into larger superstructures may give rise to unexpected collective properties. In this context it should be noted that the presently investigated (neutral) spherical species like **1a** show aggregation processes not only in solution but also under gaseous and solid-state conditions.[19]

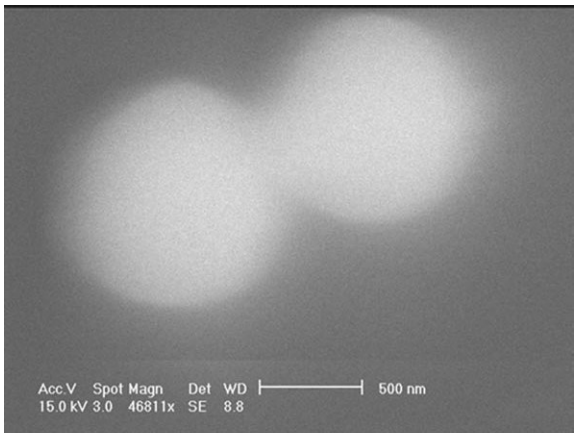

Figure 5. SEM image showing spherical supramolecular structures with radii of ≈300–350 nm formed from **2a** in ≈50 vol.% water/acetone.

4. Experimental Section

Magnetic susceptibility and magnetization measurements: These were performed on powder samples of **2** and **3** using a Quantum Design MPMS XL7 SQUID magnetometer. The data were corrected for diamagnetic contributions to the molar magnetic susceptibility using Pascal's constants.

DLS measurements: A commercial Brookhaven Instrument LLS spectrometer equipped with a solid-state laser operating at

532 nm was used.[20] The data, analyzed by the CONTIN method,[21] can be used to determine the average hydrodynamic radius R_h of the particles. The particle-size distribution in solution is obtained from a plot of $\Gamma G(\Gamma)$ versus R_h, with $\Gamma_i G(\Gamma_i)$ proportional to the angular-dependent scattered intensity of particle *i* having an apparent hydrodynamic radius $R_{h,i}$. Detailed descriptions of the DLS technique can be found in an earlier publication.[22] An aqueous solution of **2** was heated at 50 °C for two days before the measurement.

Scanning electron microscopy (SEM): A Philips XL30 ESEM was used for SEM studies of the sample solutions. The ESEM was used in SEM mode with a SE detector and set to an accelerating voltage of 20 kV with a spot size of 3.0 nm, under high-vacuum conditions. Droplets of solutions of **2** were placed onto SEM stubs, dried, and then analyzed.

*Synthesis of **2***: A solution of $CeCl_3.7H_2O$ (1.48 g, 4 mmol) in H_2O (25 mL) was added dropwise to a solution of **1** (0.5 g, 0.027 mmol) in water (75 mL) at 40 °C under stirring. The resulting mixture was stirred for 15 min, then the slight precipitate was removed by filtration and the solution was left undisturbed in an open flask. After three weeks, yellow crystals were filtered off and washed with ice-cold water. Yield: 0.15 g. Characteristic IR bands in cm^{-1} (KBr disk): 3421 (vs), 1624 (m) [$\delta(H_2O)$], 960 (w) [v(Mo=O)], 862 (m), 781 (vs) [v(Mo-O-Mo)], 617 (w), 567 (s), 426 (m). Characteristic Raman bands (solid state, KBr dilution, $\lambda_e \approx 1064$ nm; v/cm^{-1}): 968 (vs), 946 (vs) [v(Mo=O)], 837 (s), 763 (m; not present in **1**) 576 (w), 510 (m), 439 (w), 365 (m), 236 (m). Elemental analysis (%) calcd: Mo 39.8; Fe 6.2; Ce 5.2; found: Mo 40.5; Fe 7.0; Ce 4.8. Furthermore, there are extremely weak bands at 1531 [v_{as}(COO)] and 1408 cm^{-1} [v_s(COO)] present also in the reactant **1**, which correspond to a C value of ≈0.3%. This has not been considered above because the acetates are not found in the two crystal structures **2** and **3**, and due to the related error limit of the carbon analyses (small possible impurities) as well as because of the incomplete overall structure information of the capsules interior.

*Synthesis of **3***: A solution of $PrCl_3 \cdot 6H_2O$ (1.42 g, 4 mmol) in H_2O (25 mL) was added dropwise to a solution of **1** (0.5 g, 0.027 mmol) in water (75 mL) at 40 °C under stirring. The resulting mixture was stirred for 15 min, then the slight precipitate was removed by filtration and the solution was left undisturbed in an open flask. After three weeks, yellow crystals were filtered off and washed with ice-cold water. Yield: 0.13 g. Characteristic IR bands (KBr pellet): 3421 (vs), 1624 (m) [$\delta(H_2O)$], 964 (s–m), [v(Mo=O)], 860 (s–m), 783 (vs) [v(Mo-O-Mo)], 617 (w), 565 (s), 430 (w). Characteristic Raman bands (solid state, KBr dilution, $\lambda_e \approx 1064$ nm; v/cm^{-1}): 964 (vs), 949 (vs) [v(Mo=O)], 840 (s), 760 (m; not present in **1**) 576 (w), 511 (m), 441 (w), 360 (m), 234 (m). Elemental analysis (%) calcd: Mo 39.8; Fe 6.2; Pr 5.2; found: Mo 40.5; Fe 7.0; Pr 4.8 (see also above for the synthesis of **2**).

Acknowledgements

F.L.S. thanks the Fundação para a Ciência e a Tecnologia (FCT, Portugal) for the Ph.D. scholarship No. SFRH/BD/16284/2004. The authors thankMathieu Bauer MSc (Hamburg) for the ICP-MS analyses, Prof. Dr. M. Neumann and M. Prinz (Osnabrück) for the ESCA measurements, and Prof. P. Gütlich (Mainz) for the Mössbauer spectra. A.M., D.V., and D.G.K. gratefully acknowledge the financial support of the Volkswagenstiftung, while A.M., M.D., and J.v.S. acknowledge that of the Deutsche Forschungsgemeinschaft. Furthermore, A.M. thanks the Fonds der Chemischen Industrie, the German-Israeli Foundation for Scientific Research & Development, and the European Union. T.L. thanks the National Science Foundation (CHE0545983) and the Lehigh University.

[1] a) *Handbookof Porous Solids* (Eds.: F. Schüth, K. S. W. Sing, J. Weitkamp), Wiley-VCH, Heidelberg, **2002**; b) *Chemistry of Advanced Materials: An Overview* (Eds.: L. V. Interrante, M. J. Hampden-Smith), Wiley, New York, **1998**; c) *The Chemistry of Nanomaterials: Synthesis Properties and Application*s (Eds.: C. N. R. Rao, A. Müller, A. K. Cheetham), Wiley-VCH, Weinheim, Germany, **2004**; d) *Comprehensive Supramolecular Chemistry, Vol. 7, Solid-state Supramolecular Chemistry: Two- and Three-dimensional Inorganic Networks* (Eds.: J. L. Atwood et al.; Vol. Eds.: G. Alberti, T. Bein), Elsevier/Pergamon, New York, **1996**; e) For multifunctional properties, see also: E. Coronado, J. R. Galán-Mascarós, C. J. Gómez-García, V. Laukhin, *Nature* **2000**, *408*, 447–449.

[2] a) A. Müller, S. Sarkar, S. Q. N. Shah, H. Bögge, M. Schmidtmann, Sh. Sarkar, P. Kögerler, B. Hauptfleisch, A. X. Trautwein, V. Schünemann, *Angew. Chem.* **1999**, *111*, 3435–3439; *Angew. Chem. Int. Ed.* **1999**, *38*, 3238–3241; b) A. Müller, S. Q. N. Shah, H. Bögge, M. Schmidtmann, P. Kögerler, B. Hauptfleisch, S. Leiding, K. Wittler, *Angew. Chem.* **2000**, *112*, 1677–1679; *Angew. Chem. Int. Ed.* **2000**, *39*, 1614–1616; c) A. Müller, A. M. Todea, H. Bögge, J. van Slageren, M. Dressel, A. Stammler, M. Rusu, *Chem. Commun.* **2006**, 3066–3068; d) P. Gouzerh, M. Che, *Actual. Chim.* **2006**, *298*, *9*–22.

[3] a) L. Cronin in *Comprehensive Coordination Chemistry II, Vol. 7* (Eds.: J. A. McCleverty, T. J. Meyer), Elsevier, Amsterdam, **2004**, pp. 1–56; b) D. L. Long, L. Cronin, *Chem. Eur. J.* **2006**, *12*, 3698–3706; c) L. Cronin, *Angew. Chem.* **2006**, *118*, 3656–3658; *Angew. Chem. Int. Ed.* **2006**, *45*, 3576–3578; d) A. Müller, E. Krickemeyer, H. Bögge, M. Schmidtmann, F. Peters, *Angew. Chem.* **1998**, *110*, 3567–3571; *Angew. Chem. Int. Ed.* **1998**, *37*, 3360–3363; e) A. Müller, P. Kögerler, A. W. M. Dress, *Coord. Chem. Rev.* **2001**, *222*, 193–218; f) A. Müller, S. Roy, *J. Mater. Chem.* **2005**, *15*, 4673–4677; g) M. Gross, *Chem. Br.* **2003**, August, 18; h) L. Cronin, E. Diemann, A. Müller, in *Inorganic Experiments* (Ed.: J. D. Woollins), Wiley-VCH, Weinheim, Germany, **2003**, p. 340–346 (the latter reference refers to facile syntheses).

[4] a) T. Liu, B. Imber, E. Diemann, G. Liu, K. Cokleski, H. Li, Z. Chen, A. Müller, *J. Am. Chem. Soc.* **2006**, *128*, 15914–15920; see also: b) G. Liu, T. Liu, *J. Am. Chem. Soc.* **2005**, *127*, 6942–6943; c) T. Liu, *J. Am. Chem. Soc.* **2002**, *124*, 10942–10943; Corrigendum: **2004**, 126, 406; d) T. Liu, *J. Am. Chem. Soc.* **2003**, *125*, 312–313; e) G. Liu, Y. Cai, T. Liu, *J. Am. Chem. Soc.* **2004**, *126*, 16690–16691; f) G. Liu, T. Liu, *Langmuir* **2005**, *21*, 2713–2720.

[5] a) A. Müller, M. Luban, C. Schröder, R. Modler, P. Kögerler, M. Axenovich, J. Schnack, P. Canfield, S. Bud'ko, N. Harrison, *ChemPhysChem* **2001**, *2*, 517–521; b) D. Gatteschi, R. Sessoli, J. Villain, *Molecular Nanomagnets*, Oxford University Press, Oxford, **2006**; V. O. Garlea, S. E. Nagler, J. L. Zarestky, C. Stassis, D. Vaknin, P. Kögerler, D. F. McMorrow, C. Niedermayer, D. A. Ten-

nant, B. Lake, Y. Qiu, M. Exler, J. Schnack, M. Luban, *Phys. Rev. B* **2006**, *73*, 024414:1–5 and references therein.

[6] Lanthanide cations, which exhibit large coordination numbers as well as a variety of coordination geometries, play a tremendous role in polyoxometalate chemistry in that they can link polyoxometalate fragments,[7a] while their incorporation into molybdenum–oxide-based structures can even have an influence on shapes and sizes, as for instance in the case of wheel-shaped systems.[7b,8]

[7] a) See for example, M. Sadakane, M. H. Dickman, M. T. Pope, *Angew. Chem.* **2000**, *112*, 3036–3038; *Angew. Chem. Int. Ed.* **2000**, *39*, 2914–2916; C. Zhang, L. Bensaid, D. McGregor, X. Fang, R. C. Howell, B. Burton-Pye, Q. Luo, L. Todaro, L. C. Francesconi, *J. Cluster Sci.* **2006**, *17*, 389–425; M. T. Pope, A. Müller, *Angew. Chem.* **1991**, *103*, 56–70; *Angew. Chem. Int. Ed. Engl.* **1991**, *30*, 34–48; b) L. Cronin, C. Beugholt, E. Krickemeyer, M. Schmidtmann, H. Bögge, P. Kögerler, T. K. K. Luong, A. Müller, *Angew. Chem.* **2002**, *114*, 2929–2932; *Angew. Chem. Int. Ed.* **2002**, *41*, 2805–2808.

[8] A. Müller, C. Beugholt, H. Bögge, M. Schmidtmann, *Inorg. Chem.* **2000**, *39*, 3112–3113.

[9] a) H. S. M. Coxeter, *Introduction to Geometry*, 2nd ed., Wiley, New York, **1989**; b) H. S. M. Coxeter, *Regular Polytopes*, 3rd ed., Dover, New York, **1973**; c) M. O'Keeffe, B. G. Hyde, *Crystal Structures, I. Patterns and Symmetry*, Mineralogical Society of America, Washington, DC, **1996**.

[10] *Crystal data for* **2**: $H_{610}Fe_{24}Ce_8Mo_{90}O_{623}$, $M = 21678.84\ g\,mol^{-1}$, rhombohedral, space group $R\bar{3}c$, $a = 27.6346(8)$, $c = 133.355(8)$ Å, $V = 88195(5)$ Å^3, $Z = 6$, $\rho = 2.449\ g\,cm^{-3}$, $\mu = 3.151\ mm^{-1}$, $F\ (000) = 62772$, crystal size $= 0.40 \times 0.25 \times 0.02\ mm^3$. Crystals of **2** were removed from the mother liquor and immediately cooled to 188(2) K on a Bruker AXS SMART diffractometer (three-circle goniometer with 1 K CCD detector, Mo Kα radiation, graphite monochromator; hemisphere data collection in ω at 0.3° scan width in three runs with 606, 435, and 230 frames ($\Phi = 0$, 88, and 180°) at a detector distance of 5.00 cm). A total of 170077 reflections ($1.54 < \Theta < 26.99°$) were collected of which 21398 reflections were unique (R(int) = 0.067). An empirical absorption correction using equivalent reflections was performed with the program SADABS-2.10. The structure was solved with the program SHELXS-97 and refined using SHELXL-97 to $R = 0.0732$ for 16351 reflections with $I > 2\sigma(I)$, $R = 0.0977$ for all reflections; max./min. residual electron density 1.69 and $-1.12\ e\,Å^{-3}$. *Crystal data for* **3**: $H_{610}Fe_{24}Pr_8Mo_{90}O_{623}$, $M = 21685.16\ g\,mol^{-1}$, rhombohedral, space group $R\bar{3}c$, $a = 27.5804(6)$, $c = 133.318(4)$ Å, $V = 87826(4)$ Å^3, $Z = 6$, $\rho = 2.460\ g\,cm^{-3}$, $\mu = 3.208\ mm^{-1}$, $F\ (000) = 62820$, crystal size $= 0.40 \times 0.20 \times 0.11$ mm3. Crystals of **3** were removed from the mother liquor and immediately cooled to 188(2) K on a Bruker AXS SMART diffractometer (three-circle goniometer with 1 K CCD detector, Mo Kα radiation, graphite monochromator; hemisphere data collection in ω at 0.3° scan width in three runs with 606, 435, and 230 frames ($\Phi = 0$, 88, and 180°) at a detector distance of 5.00 cm). A total of 167230 reflections ($1.55 < \Theta < 26.99°$) were collected of which 21308 reflections were unique (R(int) = 0.071). An empirical absorption correction using equivalent reflections was performed with the program SADABS-2.10. The structure was solved with the program SHELXS-97 and refined using SHELXL-97 to $R = 0.1035$ for 17955 reflections with $I > 2\sigma(I)$, $R = 0.1168$ for all reflections; max./min. residual electron density 2.22 and $-1.30\ e\,Å^{-3}$. SHELXS/L, SADABS from G. M. Sheldrick, University of Göttingen, **1997**, **2003**; structure graphics with DIAMOND 2.1 from K. Brandenburg, Crystal Impact GbR, **2001**. Further details of the crystal structure investigations may be obtained from Fachinformationszentrum Karlsruhe, 76344 Eggenstein-Leopoldshafen, Germany (fax: (+49)7247–808–666; e-mail: *crysdata@fiz-karlsruhe.de*, *http://www.fiz-karlsruhe.de/ecid/Internet/en/DB/icsd/depot anforderung.html*) on quoting the deposition numbers CSD 417117 for **2** and CSD 417118 for **3**.

[11] a) A. Müller, S. K. Das, E. Krickemeyer, P. Kögerler, H. Bögge, M. Schmidtmann, *Solid State Sci.* **2000**, *2*, 847–854; b) The consideration of the capsule content $\{Mo_{18}O_{66}Ln_2(H_2O)_n\}$ is formal as nonbridging oxygen atoms are comparably strongly interacting with the atoms of the positively charged skeleton. This is a different situation to compound **4** where the encapsulated molybdate is noncovalently bonded. The small number n is included for the number of crystal water molecules with respect to the gross formula.[10]

[12] Compound **5** contains the clusters **1a** crosslinked, while the related lowering of symmetry of the space group in **5** allows a better resolution of the disorder than that of **1a**. This fact was used for obtaining the formula of **1a**: A. Müller, E. Krickemeyer, S. K. Das, P. Kögerler, S. Sarkar, H. Bögge, M. Schmidtmann, Sh. Sarkar, *Angew. Chem.* **2000**, *112*, 1674–1676; *Angew. Chem. Int. Ed.* **2000**, *39*, 1612–1614.

[13] A. Müller, S. K. Das, P. Kögerler, H. Bögge, M. Schmidtmann, A. X. Trautwein, V. Schünemann, E. Krickemeyer, W. Preetz, *Angew. Chem.* **2000**, *112*, 3555–3559; *Angew. Chem. Int. Ed.* **2000**, *39*, 3413–3417.

[14] C. Benelli, D. Gatteschi, *Chem. Rev.* **2002**, *102*, 2369–2387.

[15] a) B. K. Hodnett, *Heterogeneous Catalytic Oxidation*, Wiley, New York, **2000**; R. A. Sheldon, R. A. van Santen, *Catalytic Oxidation*, World Scientific, Singapore, **1995**; b) S. Q. Liu, D. G. Kurth, B. Bredenkotter, D. Volkmer, *J. Am. Chem. Soc.* **2002**, *124*, 12279–12287.

[16] S. Q. Liu, D. Volkmer, D. G. Kurth, *Pure Appl. Chem.* **2004**, *76*, 1847–1867.

[17] S. Q. Liu, D. Volkmer, D. G. Kurth, *Anal. Chem.* **2004**, *76*, 4579–4582.

[18] S. Polarz, B. Smarsly, C. Göltner, M. Antonietti, *Adv. Mater.* **2000**, *12*, 1503–1507.

[19] A. Müller, S. Roy, *Eur. J. Inorg. Chem.* **2005**, *18*, 3561–3570.

[20] B. Chu, *Laser Light Scattering: Basic Principles and Practice*, 2nd ed., Academic Press, New York, **1991**.

[21] S. W. Provencher, *Biophys. J.* **1976**, *16*, 27–41.

[22] G. Liu, T. Liu, S. S. Mal, U. Kortz, *J. Am. Chem. Soc.* **2006**, *128*, 10103–10110.